technologies

Article

Study of Structural, Strength, and Thermophysical Properties of $Li_{2+4x}Zr_{4-x}O_3$ Ceramics

Artem L. Kozlovskiy [1,2,3,*], Bauyrzhan Abyshev [3], Dmitriy I. Shlimas [1,3] and Maxim V. Zdorovets [1,3]

[1] Laboratory of Solid State Physics, The Institute of Nuclear Physics, Almaty 050032, Kazakhstan; shlimas@mail.ru (D.I.S.); mzdorovets@gmail.com (M.V.Z.)
[2] Institute of Geology and Oil and Gas Business, Satbayev University, Almaty 050032, Kazakhstan
[3] Engineering Profile Laboratory, L.N. Gumilyov Eurasian National University, Nur-Sultan 010008, Kazakhstan; baurzhan.abyshev@gmail.com
* Correspondence: kozlovskiy.a@inp.kz; Tel./Fax: +7-702-441-33-68

Abstract: The work is devoted to the study of technology that can be used to obtain lithium-containing ceramics of the $Li_{2+4x}Zr_{4-x}O_3$ type using the method of solid-phase synthesis combined with thermal annealing at a temperature of 1500 °C. A distinctive feature of this work is the preparation of pure Li_2ZrO_3 ceramics with a high structural ordering degree (more than 88%) and density (95–97% of the theoretical density). During the study, it was found that a change in the content of initial components for synthesis does not lead to the formation of new phase inclusions; however, an increase in the $LiClO_4 \cdot 3H_2O$ and ZrO_2 components leads to changes in the size of crystallites and dislocation density, which lead to the strengthening of ceramics to external mechanical influences. The results of the measurements of thermophysical characteristics made it possible to establish that the compaction of ceramics and a decrease in porosity lead to an increase in the thermal conductivity coefficient of 3–7%.

Keywords: lithium-containing ceramics; mechanochemical synthesis; thermal annealing; phase composition; grain sizes

Citation: Kozlovskiy, A.L.; Abyshev, B.; Shlimas, D.I.; Zdorovets, M.V. Study of Structural, Strength, and Thermophysical Properties of $Li_{2+4x}Zr_{4-x}O_3$ Ceramics. *Technologies* **2022**, *10*, 58. https://doi.org/10.3390/technologies10030058

Academic Editors: Eugene Wong, Sharon Nai and Balaguru Sethuraman

Received: 10 March 2022
Accepted: 6 May 2022
Published: 10 May 2022

1. Introduction

One of the important tasks in nuclear energy, set by the International Atomic Energy Commission, is the search for alternative ceramics to the main type, Li_4SiO_4 ceramics, which are used as tritium breeder materials in new-generation reactors, particularly in helium-cooled pebble-bed reactors [1–3]. The search for alternative materials is associated with expanding the capabilities of materials such as blankets, as well as studying the possibilities of increasing the production of tritium in the reactor itself due to transmutation reactions of the $^6Li + n \rightarrow He + T$ type and its subsequent accumulation [4,5]. At the same time, it is worth considering the fact that the short lifetime of tritium, due to rapid radioactive decay, makes its shelf life extremely limited, which leads to the need for constant reproduction of tritium in a thermonuclear reactor.

One of the ways to solve this problem is the use of lithium-containing ceramics as blanket materials, which are placed in the reactor walls for the continuous reproduction of tritium and the maintenance of thermonuclear reactions [6–8]. In this case, the ceramic material is subjected to continuous irradiation, accompanied by thermal heating and the accumulation of radiation damage associated with transmutation reactions, the main products of which are tritium and helium [9,10]. In turn, the accumulation of helium in the structure can lead to gaseous swelling of the near-surface layer of ceramics, the accumulation of stresses, and the deformations of the structure, which can subsequently lead to a decrease in strength and thermal characteristics [11–14]. In this regard, additional requirements are imposed on lithium-containing ceramics, related to their resistance, that is,

requirements not only related to their radiation resistance to helium swelling processes but also to their resistance to mechanical and thermal loads that may occur during operation.

Moreover, one of the selection criteria for lithium-containing ceramics is the choice of the oxide component, which plays an important role in determining the structural characteristics of ceramics. In particular, one of the alternative materials to classical lithium-containing ceramics of the Li_4SiO_4 type is lithium zirconate (Li_2ZrO_3)-based ceramics, which have high mechanical strength; resistance to corrosion and radiation damage; and high compatibility with various materials, which opens up prospects for their application as materials for blankets [15–17]. As is known, the main factor influencing the rate of tritium release as a result of nuclear reactions is the microstructure of ceramics, which depends not only on the choice of ceramic type but also on the conditions for their production.

The most common method to obtain Li_2ZrO_3 ceramics is the method of thermal fusion of lithium carbonate (Li_2CO_3) and zirconium dioxide (ZrO_2) at high temperatures (over 700 °C), although in a number of works, it is indicated that this method is accompanied by the production of ceramics containing amorphous inclusions, as well as impurities in the form of undissolved ZrO_2 or transitional phases of the $Li_6Zr_2O_7$ type [18–20]. At the same time, if the presence of the ZrO_2 impurity phase, as a rule, is due to an excess of the initial powders used for synthesis, then the formation of the $Li_6Zr_2O_7$ phase may be associated with the appearance of heterogeneities in the composition, leading to local variations in stoichiometry [21]. One of the alternative options for the synthesis of lithium-containing ceramics is the replacement of Li_2CO_3 with $LiClO_4 \cdot 3H_2O$, which makes it possible to obtain pure ceramics at high temperatures due to accelerated melting processes.

One of the ways to reduce the concentration of impurities is the doping of ceramics with various oxides, which leads to a decrease in the sintering temperature but, at the same time, is accompanied by the formation of two–three-phase ceramics [22–25], which have also found their application in view of the possibility of increasing the productivity of tritium release, as well as an increase in resistance to external mechanical influences. Moreover, in a number of works, it was noted that the presence of two phases leads to an increase in the resistance of ceramics to external influences, including radiation damage [26,27].

Despite a fairly large number of scientific studies aimed at studying the properties of $Li_{2+4x}Zr_{4-x}O_3$ ceramics, as well as the methods for their production, there are still many questions related to the formation of the ceramic structure and ways to get rid of impurities, as well as an increase in the lithium content in the ceramic structure, which plays a key role in the further practical application of ceramics. In this regard, the main purpose of this work was to study the structural ordering processes, as well as the mechanical and heat-conducting properties of Li_2ZrO_3 ceramics obtained by solid-state synthesis followed by thermal sintering at a temperature of 1500 °C, depending on the concentration of components in the composition of ceramics. At the same time, the features of this work that distinguish it from previous studies are as follows: Firstly, based on the results of previous studies [28], as well as a number of other studies, the annealing temperature was chosen to be much higher than (1500 °C instead of 900–1100 °C) that used in most studies, the choice of which was determined by the possibilities of the thermal annealing of defects and impurity inclusions arising during thermal sintering at temperatures below 1000 °C. Secondly, a change in the concentration of the $xLiClO_4 \cdot 3H_2O$ and $(1-x)ZrO_2$ components from x = 0.1–0.5 made it possible to evaluate the change in the properties of ceramics with different lithium content in the structure, as well as its effect on the structural, mechanical, and strength properties of ceramics.

The interest in this class of ceramics is due to their great prospects for use as nuclear materials for breeders for the purpose of breeding tritium, as well as the production of nuclear fuel and the maintenance of thermonuclear reactions. The use of oxide ceramics as nuclear materials is associated with radiation damage processes, which, as is known from the literature [29–33], can have a significant effect on the preservation of material properties, including strength characteristics and thermophysical parameters [29–33].

2. Experimental Section

$LiClO_4 \cdot 3H_2O$ and ZrO_2 powders, purchased from Sigma Aldrich (Saint Louis, MO, USA), were chosen as initial reagents for synthesis; the powder sizes were no more than 1 μm, and their chemical purity was 99.95%.

The synthesis of ceramics was carried out using the method of mechanochemical synthesis, combined with thermal annealing of the resulting ground mixtures at an annealing temperature of 1500 °C. The synthesis was carried out by varying the content of the components $xLiClO_4 \cdot 3H_2O$ and $(1-x)ZrO_2$, where x = 0.1–0.5 in order to determine the effect of changes in the concentration of the components on the structural parameters and phase composition of the studied ceramics. The grinding of samples after weighing was carried out in a PULVERISETTE 6 planetary mill (Fritsch, Germany) under the following conditions: grinding speed 400 rpm and grinding time 1 h. Thermal annealing was carried out in a muffle furnace at a temperature of 1500 °C for one hour; the heating rate was 10 °C/min, and the cooling time was 24 h.

Figure 1 shows a schematic representation of the main processes used to obtain lithium-containing ceramics, including component weighing, mechanochemical grinding, and subsequent thermal sintering at specified parameters.

Figure 1. Schematic representation of the production of $Li_{2+4x}Zr_{4-x}O_3$ ceramics.

The study of the structural parameters, as well as the phase composition of the synthesized ceramics, was carried out using the method of X-ray diffraction phase analysis. The diffraction patterns were taken in Bragg–Brentano geometry on a D8 Advance ECO powder diffractometer (Bruker, Germany). The recording conditions were as follows: 2θ = 25–75°, step 0.03°, and spectrum acquisition time at the point 1 s. An analysis of the structural parameters was carried out using the DiffracEVA v.4.2 program code, the phases were determined using the full-profile Rietveld method, and the phases were refined using the PDF-2 (2016) database.

The determination of ceramic density was carried out by analyzing changes in crystal lattice volume with further application of the obtained data in Formula (1):

$$p = \frac{1.6602 \sum AZ}{V_o}, \quad (1)$$

where V_o is the crystal lattice volume depending on the composition of the ceramics, Z is the number of atoms in a crystal cell, and A is the atomic weight of atoms.

The crystallite sizes were determined using the Scherrer method, which is based on the determination of the FHWM value depending on the angular position of the diffraction maxima.

The dislocation density was estimated using Formula (2):

$$\delta = \frac{1}{L^2} \quad (2)$$

where L is the crystallite size, determined using the Scherrer method, taking into account the contribution of reflection shape distortions.

The crystallinity degree was determined by calculating the ratio of the diffraction reflection areas to the background radiation area, which is characteristic of disordered regions in the ceramic structure.

The study of strength properties was carried out using two methods. The determination of hardness was carried out using the indentation method, which was implemented using a LECO LM 700 microhardness tester (LECO Corporation, Saint Joseph, MI, USA). A Vickers pyramid was used as an indenter, with an indenter load of 10 N.

Resistance to single compression was determined by testing the compression of samples in a press with a compression rate of 0.1 mm/min. The resistance limit was defined as the maximum pressure that the sample could withstand until cracking and partial destruction.

The study of the thermo-physical properties of the ceramics was carried out using the method of determining the temperature difference with a longitudinal heat flux through the sample during heating. The thermal conductive characteristics were evaluated using Formula (3), which makes it possible to determine the thermal conductivity coefficient.

$$\lambda = \frac{q\delta}{t_{c1} - t_{c2}}, \quad (3)$$

where q is the heat flux density, W/m^2; t_{c1} and t_{c2} are the temperatures on both sides of the sample, K; and δ is the thickness of the sample, m. The temperature difference was measured using a KIT-800 instrument (Moscow, Russia).

3. Results and Discussion

Figure 2 shows the results of the X-ray diffraction phase analysis of the studied ceramics regarding the concentration of the components. A full-profile analysis of the obtained diffraction patterns made it possible to establish that the main reflections are characteristic of the Li_2ZrO_3 monoclinic phase (PDF-01-070-8744) with C2/2(15) spatial syngony. According to the results in [28], thermal annealing at temperatures above 900 °C leads to the displacement of LiO and ZrO_2 impurity phases from the ceramic structure, and a further increase in the annealing temperature leads to the ordering of the structural parameters (lattice parameter and crystallinity degree) and a change in the grain size associated with their coarsening and increase in density. An analysis of the obtained diffraction patterns indicated that a change in the component concentrations in the composition of the ceramics, as well as subsequent thermal annealing, does not lead to the formation of new phases, as evidenced by the absence of new reflections in the diffraction patterns. Unlike commercial samples of Li_2ZrO_3 ceramics, in the structure of which, according to the data in [18], the presence of impurity phases of the initial ZrO_2 and Li_2CO_3 powders was observed, impurity inclusions were not found in the studied samples obtained at a temperature of 1500 °C. At the same time, the data of a comparative analysis of the areas of diffraction reflections and background radiation indicate a high crystallinity degree of the samples (more than 85%), which varies depending on the content of the components. Moreover, the content of ZrO_2 impurity inclusions in the structure of Li_2ZrO_3 ceramics was reported in [19], the presence of which is due to manufacturing processes. Moreover, in most known works [20], thermal sintering occurs at temperatures of 700–1100 °C. The main changes in the diffraction patterns are mainly associated with changes in the intensity of reflections and their width; this is characterized by a change in the size of crystallites, as well as a shift of reflections to the region of large angles, which is typical for a change in crystal lattice parameters. For comparison, the changes in the main reflections and their positions are presented, according to which, an increase in the concentration of the $LiClO_4$ component in the initial mixture leads to a decrease in the intensity of reflections and their shift. At the same time, the greatest changes are observed for ceramics with a content of x = 0.4–0.5. Such a shift may be due to the substitution of zirconium ions (13.9 Å), which have a radius larger than that of lithium ions (7.1 Å). An increase in the lithium concentration in the structure, in turn, does not lead to the formation of impurity phases, and a decrease in the intensity of reflections and a change in their width (FWHM) indicate changes in the size of

crystallites and their fragmentation, which, in turn, lead to an increase in the dislocation density due to an increase in grain boundaries. A change in the positions of reflections, including their shift to the large angle region, as is known, leads to a decrease in crystal lattice parameters, which can be due to several factors: the processes of substitution of atoms of one type for atoms of another type; the deformation processes of crystal lattice compression, leading to its compaction; and relaxation processes associated with changes in point defect concentration in the composition of ceramics as a result of external influences. It is also worth noting that the change in the crystal lattice parameters may be due to the effect associated with a change in the component concentration of O-vacancies. An increase in the lithium concentration in the structure can also lead to the formation of additional vacancy defects, which are formed as a result of the partial breaking of Zr-O chemical bonds. In this case, part of the free oxygen can be displaced from the structure during thermal annealing.

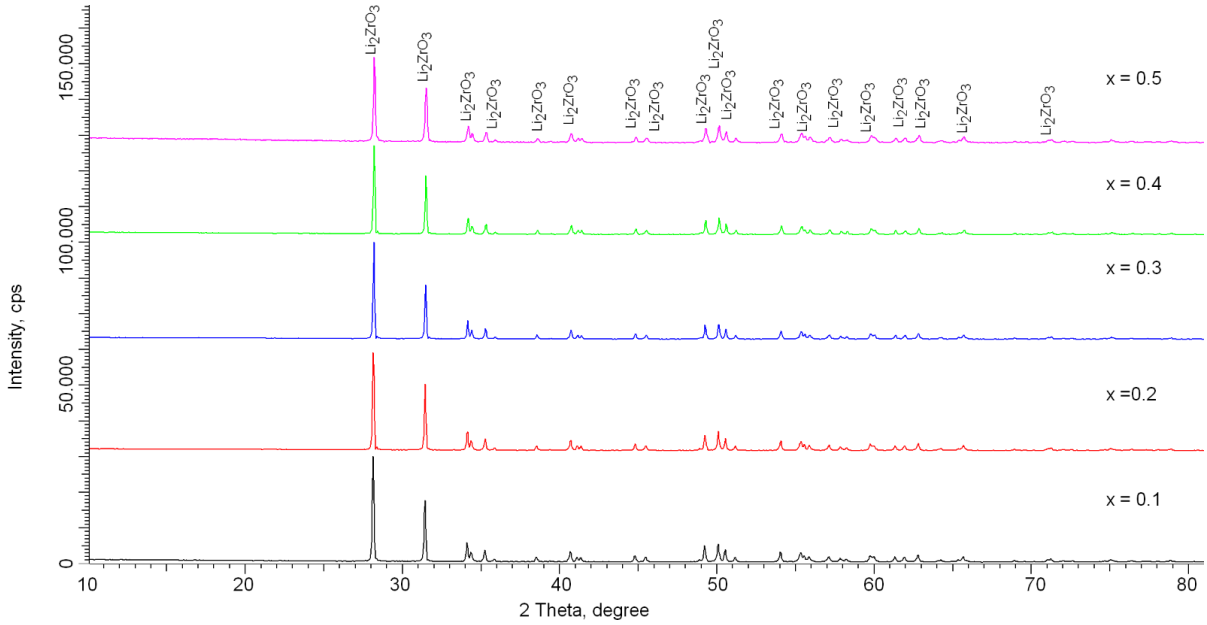

Figure 2. X-ray diffraction patterns of the studied ceramics.

When estimating the shape of the diffraction reflection lines, it was determined that deformation effects associated with the structure distortion make a very small contribution to the change in structural parameters (no more than 5–10% according to the Williamson–Hall method), and the change in the shape of reflections is mostly due to size effects, leading to a change in the dislocation density.

Relaxation processes also do not make a large contribution to the change in structural parameters, since the crystallinity degree does not increase with changes in component concentrations, but it has a slight downward trend, which indicates the absence of defect annealing processes.

Based on this, it was assumed that the main changes in diffraction reflections associated with a maxima position shift to the large angle region are due to the effects of the substitution of zirconium ions by lithium ions in the lattice sites with an increase in the lithium-containing component concentration in the ceramic during its synthesis.

Table 1 presents the results of evaluating the structural parameters, as well as the crystallinity degree of the samples under study. It can be seen from the data presented that an increase in the X component content leads to a decrease in the crystal lattice parameters. However, a change in the crystal lattice parameters leads to a slight decrease in the structural ordering degree, which may be due to the partial replacement of zirconium ions by lithium ions at the lattice sites, as well as the fragmentation of crystallites, the size of which also decreases. In turn, a decrease in the size of crystallites leads to an increase in

the dislocation density, which plays an important role in increasing the strength properties.

Table 1. Unit-cell parameters and crystallinity characteristics for Li_2ZrO_3 ceramics.

Parameter	Content of $LiClO_4 \cdot 3H_2O$ Component				
	0.1	**0.2**	**0.3**	**0.4**	**0.5**
Li_2ZrO_3 monoclinic phase (PDF-01-070-8744) (a_0 = 5.42660 Å, b_0 = 9.03100 Å, c_0 = 5.42270 Å, β_0 = 112.720°, V_0 = 245.13 Å^3) Crystal lattice parameters, Å	a = 5.3915 ± 0.0011, b = 9.0363 ± 0.0014, c = 5.4216 ± 0.0021, β = 112.609°	a = 5.3829 ± 0.0017, b = 9.0291 ± 0.0022, c = 5.4173 ± 0.0024, β = 112.564°	a = 5.3786 ± 0.0018, b = 9.0061 ± 0.0015, c = 5.4056 ± 0.0022, β = 112.474°	a = 5.3691 ± 0.0016, b = 8.9989 ± 0.0013, c = 5.3855 ± 0.0014, β = 112.384°	a = 5.3617 ± 0.0015, b = 8.9901 ± 0.0023, c = 5.3761 ± 0.0017, β = 112.010°
Crystal volume, Å^3	243.84 ± 0.19	243.14 ± 0.16	241.96 ± 0.12	240.61 ± 0.15	240.25 ± 0.14
Crystallinity degree, % (structural ordering value)	90.2 ± 0.4	89.3 ± 0.5	88.7 ± 0.3	88.6 ± 0.5	88.0 ± 0.7
Crystallite size, nm (size determined using the Scherer equation)	80.2 ± 2.5	76.4 ± 2.6	76.3 ± 2.8	72.2 ± 2.4	65.5 ± 2.1
Dislocation density, 10^{10} 1/cm^2	0.155	0.171	0.172	0.191	0.233

Figure 3 shows the assessment results of changes in the crystal lattice parameters depending on the X component concentration in comparison with the reference values of the parameters for the Li_2ZrO_3 phase (PDF-01-070-8744) (a_0 = 5.42660 Å, b_0 = 9.03100 Å, c_0 = 5.42270 Å, β_0 = 112.720°, and V_0 = 245.13 Å^3).

The results of changes in the structural parameters (Figure 3) for high annealing temperatures are in good agreement with the results in [34], according to which, at high annealing temperatures, an anisotropic change in the crystal lattice parameters was observed due to thermal effects, as well as the difference in cationic radii. In this case, changes in the parameter *a* depending on the content of the component have an isotropic nature of distortions, while the parameters *b* and *c* change anisotropically, which may be due to the difference in the filling of lattice sites, as well as inhomogeneity in the replacement of zirconium ions by lithium ions.

A decrease in the crystal lattice parameters, as is known, leads to a decrease in its volume and, consequently, to a decrease in porosity and an increase in the density of ceramics. Figure 4 shows the results of changes in the density and porosity of the ceramics depending on the X component concentration. A change in density, including its decrease at high annealing temperatures of 1500 °C, is due to the fact that with a change in the components used for synthesis, by varying them with a subsequent increase in $LiClO_4 \cdot 3H_2O$, the crystal lattice volume decreases, which leads to ceramic compaction. At the same time, the difference from the density values presented in [28], which are close to the theoretical values, is that, at high lithium concentrations, there is an overall increase in the lattice volume, which leads to lower ceramic density values.

As can be seen from the data presented, a change in the crystal lattice parameters leads to the compaction of ceramics, as well as the approximation of the experimentally obtained density values to the theoretical value (95–97%). In this case, porosity decreases from 4.1% to 2.6%, with an increase in the X component, which, in turn, results in the ceramics strengthening to mechanical stress.

Figure 5 shows the measurement results of the ceramics' single compression resistance. The change in the resistance value depending on the concentration of X varies in the range from 29.3 to 38.4 N, while for concentrations X = 0.4–0.5, an increase in resistance of 25–30% is observed. Such an increase in single compression resistance is due to an increase in the density of the ceramics, as well as a change in the dislocation density, which leads to a strengthening effect and an increase in fracture resistance. A comparative analysis with the known literature data on measurements of resistance to single compression, taken from [20,35,36], indicated that the synthesized ceramics have an increased resistance to mechanical stress, as well as greater strength. At the same time, as shown in [30], in which

the properties of two-component Li_4SiO_4-Li_2ZrO_3 ceramics were studied, an increase in density led to an increase in strength, which confirms the obtained results. The authors found that an increase in the resistance of ceramics to mechanical stress was not only due to an increase in density but also due to an increase in the content of Li_2ZrO_3 in the composition of the ceramics. A similar effect was also observed in [36], where it was shown that a change in component content in the composition of ceramics leads to an increase in resistance to mechanical stress.

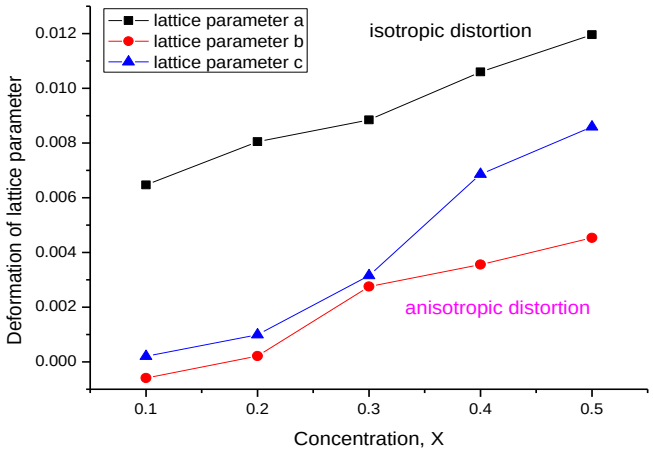

(**a**)

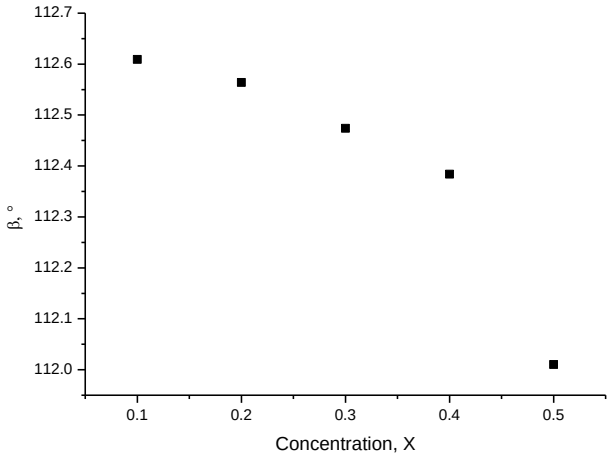

(**b**)

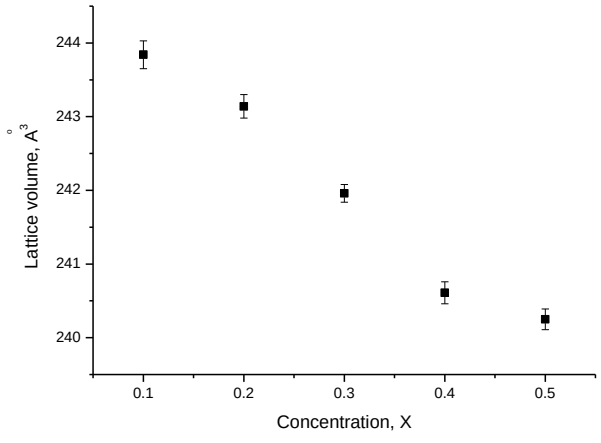

(**c**)

Figure 3. (**a**) Results of crystal lattice deformation; (**b**) results of beta angle deformation; (**c**) results of crystal lattice volume deformation.

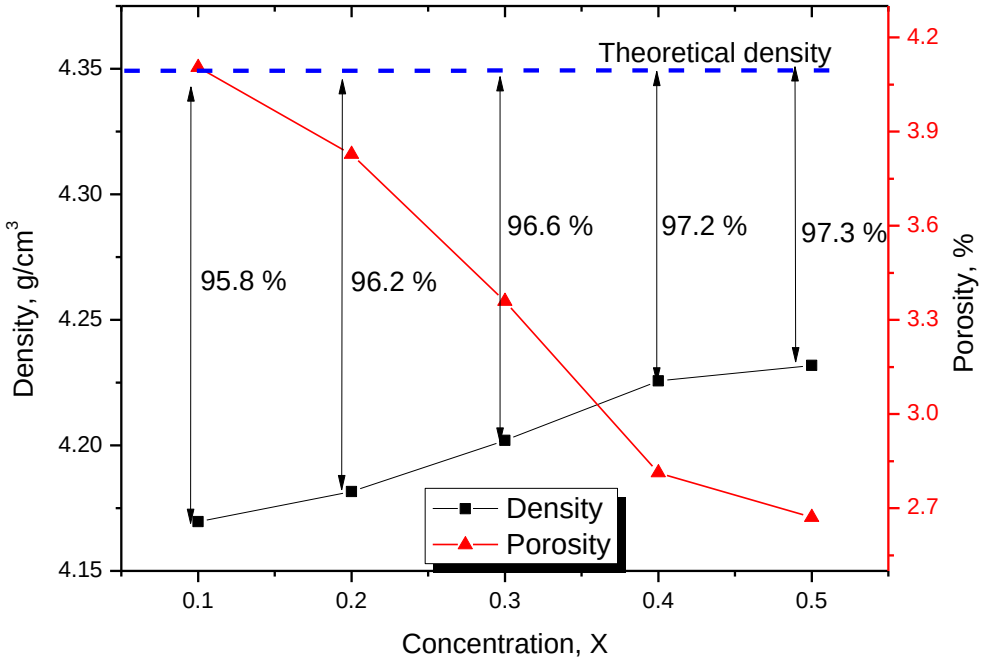

Figure 4. Ceramic density and porosity change results.

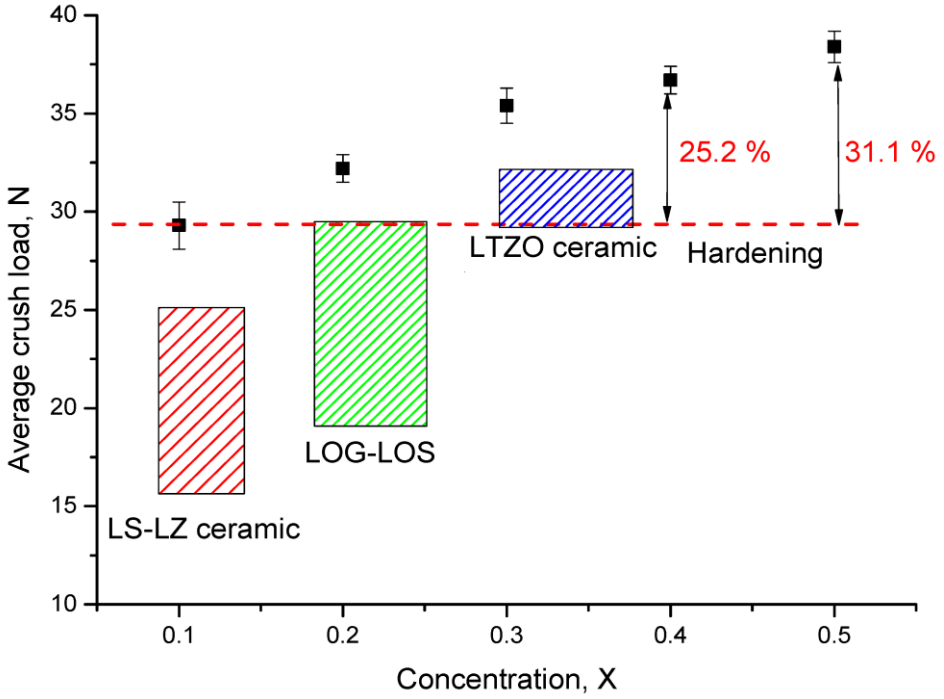

Figure 5. Results of strength measurements for single compression resistance.

As can be seen from the presented data on changes in the hardness value of the surface layer of ceramics, an increase in dislocation density leads to an increase in resistance to mechanical stress. At the same time, in the case of component concentrations of X = 0.4–0.5, the ratio of dislocation density to hardening is 3:1. The hardening effect is due to the creation of additional obstacles to the propagation of microcracks due to the high density of dislocations, which leads to an increase in resistance to mechanical stress. Moreover, an important role in strengthening is played by a decrease in the porosity of the ceramics and an increase in density; this causes a decrease in the concentration of disordered structural inclusions, which, in turn, leads to the strengthening of ceramics.

The results of the ceramic hardness obtained by indentation are shown in Figure 6.

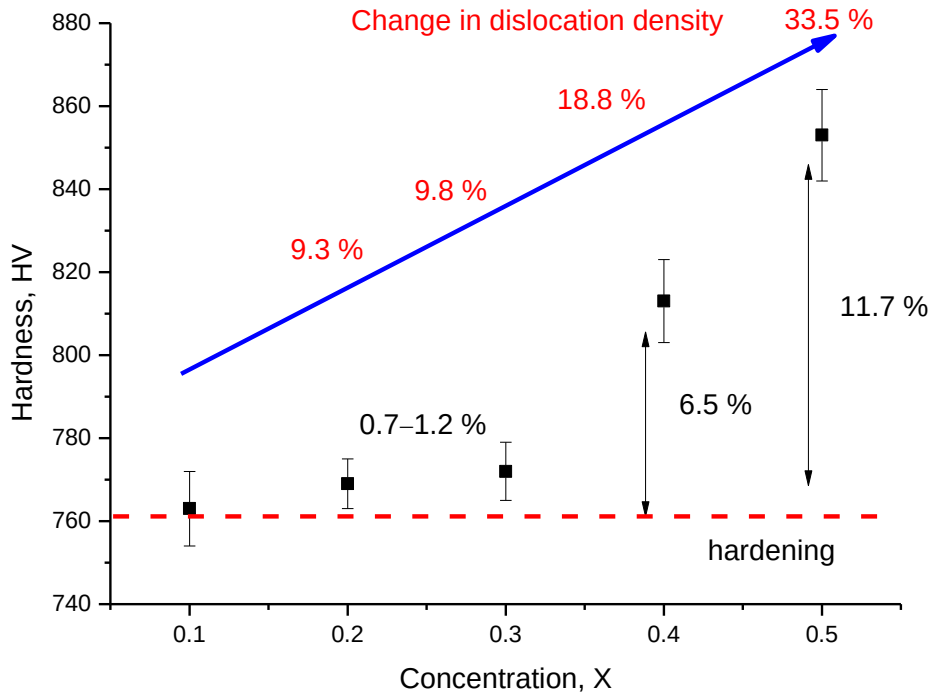

Figure 6. Ceramic hardening results depending on the concentration of component X.

The important characteristics for the determination of the operational parameters of lithium-containing ceramics are their thermophysical parameters, which play an important role in the processes of heat transfer and heat removal. Figure 7 shows the results of the change in the thermal conductivity coefficient depending on the concentration of the X component.

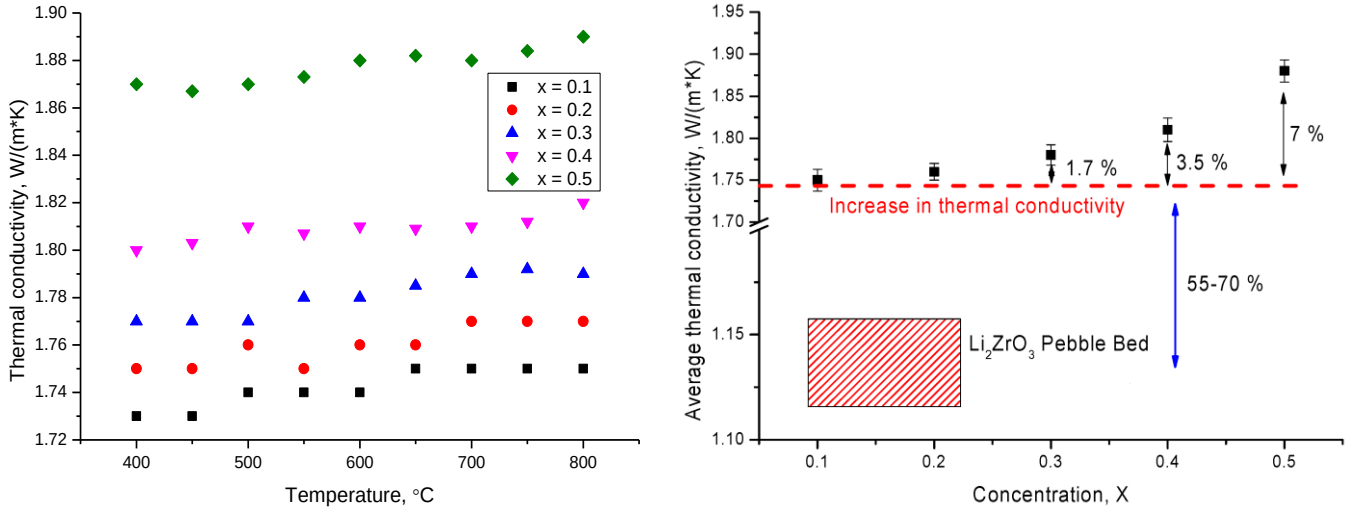

(**a**) (**b**)

Figure 7. (**a**) Dependences of the change in the thermal conductivity coefficient on temperature; (**b**) results of the change in the average value of the thermal conductivity coefficient.

As can be seen from the data presented in Figure 7a, the value of the thermal conductivity coefficient in a wide measured temperature range remains almost unchanged, with a slight increase in thermal conductivity (no more than 0.5%) at elevated measurement temperatures. At the same time, the dependences obtained indicate a high stability of thermal conductivity over the entire temperature range. A comparative diagram of the average value of thermal conductivity shows that a change in the X component concentration leads

to an increase in thermal conductivity of 3.5–7%, which indicates an increase in thermal conductivity due to structural changes, as well as a decrease in porosity. For example, as a comparison, Figure 7b shows the results of the thermal conductivity for Li_2ZrO_3 used as a blanket material [37]. According to this work, the change in thermal conductivity is influenced by two factors that are associated with heat transfer and heat transfer processes, as well as the contact area. In our case, the contact area was the same for all the samples under study; thus, the main changes are associated with the processes of heat transfer and heat transfer, which directly depend on the structure of the ceramics, as well as porosity. A decrease in porosity as a result of a change in the X component concentration leads to an increase in heat transfer and, accordingly, in the thermal conductivity. It should be noted that such a significant difference from the results in [32] is due to the fact that the studied ceramics in this work were highly porous samples with a packing density of 1.921 (at a density of 3.1 g/cm^3, 53.4% of the theoretical value).

4. Conclusions

In conclusion, the results of the research can be summarized as follows:

1. The proposed conditions to obtain Li_2ZrO_3 ceramics with different contents of the initial components $xLiClO_4 \cdot 3H_2O$ and $(1-x)ZrO_2$ (x = 0.1–0.5) at an annealing temperature of 1500 °C make it possible to obtain highly ordered pure ceramics with a monoclinic phase (Li_2ZrO_3) and a density close to the theoretical value (95–97%).
2. The decrease in the crystal lattice parameters for the Li_2ZrO_3 monoclinic phase is due to the substitution of zirconium ions (atomic radius = 13.9 Å) by lithium ions (atomic radius = 7.1 Å), and it indicates an increase in lithium concentration in the ceramic structure. At the same time, changes in the crystal lattice parameters depending on the X component concentration are anisotropic.
3. A change in the X component content leads to an increase in the dislocation density, a change in which leads to the strengthening of ceramics and an increase in resistance to mechanical stress and cracking.
4. An increase in the density of ceramics, as well as a decrease in density, leads to an increase in the thermal conductivity coefficient of 3.5–7%.

Author Contributions: Conceptualization, M.V.Z., B.A. and A.L.K.; methodology, B.A., D.I.S. and A.L.K.; formal analysis, D.I.S. and M.V.Z.; investigation, B.A., A.L.K. and M.V.Z.; resources, M.V.Z.; writing—original draft preparation, review, and editing, B.A., M.V.Z. and A.L.K.; visualization, M.V.Z.; supervision, M.V.Z. All authors have read and agreed to the published version of the manuscript.

Funding: This research was funded by the Science Committee of the Ministry of Education and Science of the Republic of Kazakhstan (No. BR11765580).

Institutional Review Board Statement: Not applicable.

Informed Consent Statement: Not applicable.

Data Availability Statement: Not applicable.

Conflicts of Interest: The authors declare that they have no conflict of interest.

References

1. Jiang, S.; Tu, J.; Yang, X.; Gui, N. A review of pebble flow study for pebble bed high temperature gas-cooled reactor. *Exp. Comput. Multiph. Flow* **2019**, *1*, 159–176. [CrossRef]
2. Piazza, G.; Reimann, J.; Knitter, E.; Roux, N.; Lulewicz, J.D. Characterisation of ceramic breeder materials for the helium cooled pebble bed blanket. *J. Nucl. Mater.* **2002**, *307*, 811–816. [CrossRef]
3. Moscato, I.; Barucca, L.; Ciattaglia, S.; D'Aleo, F.; Di Maio, P.A.; Federici, G.; Tarallo, A. Progress in the design development of EU DEMO helium-cooled pebble bed primary heat transfer system. *Fusion Eng. Des.* **2019**, *146*, 2416–2420. [CrossRef]
4. Zhang, G.; Chen, J.; Tang, G.; Gledenov, Y.M.; Sedysheva, M.; Khuukhenkhuu, G. Measurement of differential and angle-integrated cross sections of the 6Li (n, t) 4He reaction in the MeV neutron energy range. *Nucl. Instrum. Methods Phys. Res. Sect. A Accel. Spectrometers Detect. Assoc. Equip.* **2006**, *566*, 615–621. [CrossRef]

5. Biersack, J.P.; Fink, D. Observation of the blocking effect after 6Li (n, t) 4He reactions with thermal neutrons. *Nucl. Instrum. Methods* **1973**, *108*, 397–399. [CrossRef]
6. Dang, C.; Yang, M.; Gong, Y.; Feng, L.; Wang, H.; Shi, Y.; Shi, Q.; Qi, J.; Lu, T. A promising tritium breeding material: Nanostructured $2Li_2TiO_3$-Li_4SiO_4 biphasic ceramic pebbles. *J. Nucl. Mater.* **2018**, *500*, 265–269. [CrossRef]
7. Hong, M.; Zhang, Y.; Mi, Y.; Xiang, M.; Zhang, Y. Fabrication and characterization of Li_2TiO_3 core–shell pebbles with enhanced lithium density. *J. Nucl. Mater.* **2014**, *445*, 111–116. [CrossRef]
8. Chen, R.; Yang, M.; Shi, Y.; Wang, H.; Guo, H.; Zeng, Y.; Qi, J.; Shi, Q.; Liao, Z.; Lu, T. Development of an advanced core-shell ceramic pebble with Li_4TiO_4 pure phase core and Li_2TiO_3 nanostructured shell by a physical coating method. *J. Nucl. Mater.* **2019**, *520*, 252–257. [CrossRef]
9. Xiao, C.; Gao, X.; Kobayashi, M.; Kawasaki, K.; Uchimura, H.; Toda, K.; Kang, C.; Chen, X.; Wang, H.; Peng, S.; et al. Tritium release kinetics in lithium orthosilicate ceramic pebbles irradiated with low thermal-neutron fluence. *J. Nucl. Mater.* **2013**, *438*, 46–50. [CrossRef]
10. Leys, J.M.; Zarins, A.; Cipa, J.; Baumane, L.; Kizane, G.; Knitter, R. Radiation-induced effects in neutron-and electron-irradiated lithium silicate ceramic breeder pebbles. *J. Nucl. Mater.* **2020**, *540*, 152347. [CrossRef]
11. Shlimas, D.I.; Zdorovets, M.V.; Kozlovskiy, A.L. Synthesis and resistance to helium swelling of Li_2TiO_3 ceramics. *J. Mater. Sci. Mater. Electron.* **2020**, *3*, 12903–12912. [CrossRef]
12. Blynskiy, P.; Chikhray, Y.; Kulsartov, T.; Gabdullin, M.; Zaurbekova, Z.; Kizane, G.; Kenzhin, Y.; Tolenova, A.; Nesterov, E.; Shaimerdenov, A. Experiments on tritium generation and yield from lithium ceramics during neutron irradiation. *Int. J. Hydrogen Energy* **2021**, *46*, 9186–9192. [CrossRef]
13. Kulsartov, T.; Tazhibayeva, I.; Gordienko, Y.; Chikhray, E.; Tsuchiya, K.; Kawamura, H.; Kulsartova, A. Study of tritium and helium release from irradiated lithium ceramics Li_2TiO_3. *Fusion Sci. Technol.* **2011**, *60*, 1139–1142. [CrossRef]
14. Ba, J.; Zeng, R.; Yan, X.; Li, R.; Wu, W.; Li, F.; Xiang, X.; Meng, D.; Tang, T. Long-term helium bubble evolution in sequential He^+ and H^+ irradiated Li_4SiO_4. *Ceram. Int.* **2021**, *47*, 32310–32317. [CrossRef]
15. Zhao, M.; Memon, M.Z.; Ji, G.; Yang, X.; Vuppaladadiyama, A.K.; Song, Y. Alkali metal bifunctional catalyst sorbents enabled biomass pyrolysis for enhanced hydrogen production. In this study, Li_2ZrO_3, Li_4SiO_4, and Na_2ZrO_3 were selected as catalystsorbent bifunctional materials to enhance the pyrolysis of sawdust. *TIDEE TERI Inf. Dig. Energy Environ.* **2021**, *20*, 52.
16. Roux, N.; Abassin, J.J.; Briec, M.; Cruz, D.; Flament, T.; Schuster, I. Compatibility behavior of beryllium with $LiAlO_2$ and Li_2ZrO_3 ceramics, with 316 L and 1.4914 steels in SIBELIUS. *J. Nucl. Mater.* **1992**, *191*, 168–172. [CrossRef]
17. Ma, J.; Fu, Z.; Liu, P.; Tang, X. Microwave dielectric properties of low-fired Li_2ZrO_3–ZnO composite ceramics. *J. Mater. Sci. Mater. Electron.* **2016**, *27*, 232–236. [CrossRef]
18. Avila, R.E.; Peña, L.A.; Jiménez, J.C. Surface desorption and bulk diffusion models of tritium release from Li_2TiO_3 and Li_2ZrO_3 pebbles. *J. Nucl. Mater.* **2010**, *405*, 244–251. [CrossRef]
19. Rasneur, B.; Thevenot, G.; Bouilloux, Y. Irradiation behavior of $LiAlO_2$ and Li_2ZrO_3 ceramics in the ALICE 3 experiment. *J. Nucl. Mater.* **1992**, *191–194*, 243–247. [CrossRef]
20. Hoshino, T. Pebble fabrication of super advanced tritium breeders using a solid solution of $Li_{2+x}TiO_{3+y}$ with Li_2ZrO_3. *Nucl. Mater. Energy* **2016**, *9*, 221–226. [CrossRef]
21. Yasnó, J.P.; Conconi, S.; Visintin, A.; Suárez, G. Non-isothermal reaction mechanism and kinetic analysis for the synthesis of monoclinic lithium zirconate (m-Li_2ZrO_3) during solid-state reaction. *J. Anal. Sci. Technol.* **2021**, *12*, 15. [CrossRef]
22. Yang, M.; Gong, Y.; Ran, G.; Wang, H.; Chen, R.; Huang, Z.; Shi, Q.; Chen, X.; Lu, T.; Xiao, C. Tritium release behavior of Li_4SiO_4 and Li_4SiO_4+ 5 mol% TiO_2 ceramic pebbles with small grain size. *J. Nucl. Mater.* **2019**, *514*, 284–289. [CrossRef]
23. Yang, M.; Ran, G.; Wang, H.; Dang, C.; Huang, Z.; Chen, X.; Lu, T.; Xiao, C. Fabrication and tritium release property of Li_2TiO_3-Li_4SiO_4 biphasic ceramics. *J. Nucl. Mater.* **2018**, *503*, 151–156. [CrossRef]
24. Kulsartov, T.; Zaurbekova, Z.; Knitter, R.; Shaimerdenov, A.; Chikhray, Y.; Askerbekov, S.; Akhanov, A.; Kenzhina, I.; Kizane, G.; Kenzhin, Y.; et al. Studies of two-phase lithium ceramics Li_4SiO_4-Li_2TiO_3 under conditions of neutron irradiation. *Nucl. Mater. Energy* **2022**, *30*, 101129. [CrossRef]
25. Qi, Q.; Wang, J.; Zhou, Q.; Zhang, Y.; Zhao, M.; Gu, S.; Nakata, M.; Zhou, H.; Oya, Y.; Luo, G.-N. Comparison of tritium release behavior in Li_2TiO_3 and promising core-shell Li_2TiO_3–Li_4SiO_4 biphasic ceramic pebbles. *J. Nucl. Mater.* **2020**, *539*, 152330. [CrossRef]
26. Yang, M.; Zhao, L.; Ran, G.; Gong, Y.; Wang, H.; Peng, S.; Xiao, C.; Lu, T. Tritium release behavior of Li_2TiO_3 and $2Li_2TiO_3$-Li_4SiO_4 biphasic ceramic pebbles fabricated by microwave sintering. *Fusion Eng. Des.* **2021**, *168*, 112390. [CrossRef]
27. Zhou, Q.; Togari, A.; Nakata, M.; Zhao, M.; Sun, F.; Xu, Q.; Oya, Y. Release kinetics of tritium generation in neutron irradiated biphasic Li_2TiO_3–Li_4SiO_4 ceramic breeder. *J. Nucl. Mater.* **2019**, *522*, 286–293. [CrossRef]
28. Zdorovets, M.V.; Kozlovskiy, A.L.; Abyshev, B.; Yansepbayev, T.A.; Uzbekgaliyev, R.U.; Shlimas, D.I. Study of Phase Formation Processes in Li_2ZrO_3 Ceramics Obtained by Mechanochemical Synthesis. *Crystals* **2022**, *12*, 21. [CrossRef]
29. Kuzovkov, V.N.; Popov, A.I.; Kotomin, E.A.; Monge, M.A.; Gonzales, R.; Chen, Y. Kinetics of nanocavity formation based on F-center aggregation in thermochemically reduced MgO single crystals. *Phys. Rev. B* **2001**, *64*, 064102. [CrossRef]
30. Lushchik, A.; Feldbach, E.; Kotomin, E.A.; Kudryvtseva, I.; Kuzovkov, V.N.; Popov, A.I.; Seeman, V.; Shablonin, E. Distinctive features of diffusion-controlled radiation defect recombination in stoichiometric magnesium aluminate spinel single crystals and transparent polycrystalline ceramics. *Sci. Rep.* **2020**, *10*, 7810. [CrossRef]

31. Kotomin, E.A.; Kuzovkov, V.N.; Popov, A.I. The kinetics of defect aggregation and metal colloid formation in ionic solids under irradiation. *Radiat. Eff. Defects Solids* **2001**, *155*, 113–125. [CrossRef]
32. Klym, H.; Karbovnyk, I.; Piskunov, S.; Popov, A.I. Positron Annihilation Lifetime Spectroscopy Insight on Free Volume Conversion of Nanostructured $MgAl_2O_4$ Ceramics. *Nanomaterials* **2021**, *11*, 3373. [CrossRef] [PubMed]
33. Klym, H.; Ingram, A.; Shpotyuk, O.; Hadzaman, I.; Solntsev, V.; Hotra, O.; Popov, A.I. Positron annihilation characterization of free volume in micro-and macro-modified $Cu_{0.4}Co_{0.4}Ni_{0.4}Mn_{1.8}O_4$ ceramics. *Low Temp. Phys.* **2016**, *42*, 601–605. [CrossRef]
34. Heiba, Z.; El-Sayed, K. Structural and anisotropic thermal expansion correlation of Li_2ZrO_3 at different temperatures. *J. Appl. Crystallogr.* **2002**, *35*, 634–636. [CrossRef]
35. Rao, J.G.; Mazumder, R.; Bhattacharyya, S.; Chaudhuri, P. Fabrication of Li_4SiO_4-Li_2ZrO_3 composite pebbles using extrusion and spherodization technique with improved crush load and moisture stability. *J. Nucl. Mater.* **2018**, *514*, 321–333.
36. Leys, O.; Kolb, M.H.H.; Pucci, A.; Knitter, R. Study of lithium germanate additions to advanced ceramic breeder pebbles. *J. Nucl. Mater.* **2019**, *518*, 234–240. [CrossRef]
37. Enoeda, M.; Ohara, Y.; Roux, N.; Ying, A.; Pizza, G.; Malang, S. Effective Thermal Conductivity Measurement of the Candidate Ceramic Breeder Pebble Beds by the Hot Wire Method. *Fusion Technol.* **2001**, *39*, 612–616. [CrossRef]